Songklanakarin J. Sci. Technol.
43 (5), 1317-1328, Sep. - Oct. 2021

http://www.sjst.psu.ac.th

*Original Article*

# Shoulder Angle Measurement (SAM) system for home-based rehabilitation using computer vision with a web camera

Sunthorn Rungruangbaiyok, Rakkrit Duangsoithong, and Kanadit Chetpattananondh*

*Department of Electrical Engineering, Faculty of Engineering,*
*Prince of Songkla University, Hat Yai, Songkhla, 90112 Thailand*

Received: 21 April 2020; Revised: 21 August 2020; Accepted: 25 October 2020

## Abstract

Most of the patients suffering from shoulder movement impairment have some problems in daily life. Consequently, shoulder movement rehabilitation plays an important role for them and needs to be evaluated in continued treatments of the shoulder. In addition to the cost of treatment, the travel expenses to visit a hospital are also increasing. This paper proposes a shoulder angle measurement (SAM) system using computer vision with a web camera. The system detects arm in an image and calculates active shoulder angle movement. A correlation analysis of the measured shoulder angle between the SAM system and two devices, namely ATAN Scale (Adapted Thai Arthrometric Navigator Scale) and a goniometer, was performed. The Pearson correlations between the SAM system and the two devices were close to one. The maximum full-scale errors were 5.03 and 3.69 on comparing to the ATAN Scale and the goniometer, respectively.

**Keywords**: shoulder angle measurement, image detection, rehabilitation, TAN Scale, goniometer

## 1. Introduction

Shoulder rehabilitation is used for patients who have problems in the shoulder joint, with dysfunctions such as frozen shoulder, shoulder tendinitis or shoulder muscle weakness. In addition, postoperative breast cancer patients may get this type of problems. Currently, the number of cancer patients is increasing. The postoperative patients may have an impaired shoulder movement problem (Box, Reul-Hirche, Bullock-Saxton, & Furnival, 2002; Hidding, Beurskens, van der Wees, van Laarhoven, & Nijhuis-van der Sanden, 2014; Flores & Dwyer, 2014). Shoulder-arm function 6 weeks after surgery can predict long-term shoulder dysfunction substantially (Kootstra *et al.*, 2013). Therefore, the patients should receive shoulder rehabilitation immediately after the surgery, especially within 6 weeks after surgery. According to the hospital's Clinical Practice Guidelines on Breast Cancer, all patients should have follow-up in rehabilitation program at 1 day, 1 month, and 6 months after surgery (de Carlos-Iriarte *et al.*, 2019). Furthermore, if the patients have been monitored for treatment more frequently, the results from rehabilitation of the shoulder movement tend to improve rapidly. Hence, shoulder movement rehabilitation is crucial. The impaired shoulder movement patients need to be evaluated and treated by a physician or physical therapist continuously. Besides, the cost of treatment and the travel expenses for treatment at the hospital are both increasing. Consequently, a technique for the remote measurement of shoulder movement, for evaluating and monitoring, should be developed.

In general, the physical therapist measures both passive and active shoulder ranges of motion by using a goniometer (Dougherty, Walmsley, & Osmotherly, 2015). However, such use of a goniometer requires practical skills and anatomical knowledge. Therefore, angle measurement devices have been developed for ease of use that does not require special measuring skills, implemented with a smartphone (Chiensriwimol, Chan, Mongkolnam, & Mekhora, 2017; Ongvisatepaiboon, Chan, & Vanijja, 2015; Yodpijit *et al.*, 2018), or with Kinect or RGBD camera (Cao, Simon, Wei, & Sheikh, 2017; Ghazal & Khan, 2018; Huang *et al.*,2014; Huber, Leeser, Sternad & Seitz, 2015; Huber, Seitz, Leeser, & Sternad, 2014; Kumar, Muknahallipatna, McInroy, McKenna, & Franc, 2017; Mangal, Pal, & Khosla, 2017; Matsen III,

*Corresponding author
Email address: kanadit.c@psu.ac.th

Lauder, Rector, Keeling, & Cherones, 2016). Then the patient could measure angle of shoulder movement without a specialist, at home or at the primary hospital.

Evaluation of frozen shoulder is difficult because the specialist with an efficient tool are not enough. The number of patients who have impaired shoulder movement problem can increase. Consequently, Thai Arthrometric Navigator Scale (TAN Scale) has been invented to measure the angle of shoulder movement without need for a specialist. It has been developed by the National Cancer Institute of Thailand (NCI) to solve the problem discussed above (National Cancer Institute, Department of Medical Services Ministry of Public Health Thailand [NCI], 2020). The TAN Scale characteristic is a half-circular chart that demonstrates an angle along its radius. The range of angles is from 90-degree to 180-degree, clockwise and counter-clockwise. Patients can measure shoulder angle movement by standing at the center point of the TAN Scale and moving an arm parallel with the chart, as shown in Figure 1 (NCI, 2020). Nevertheless, the TAN Scale has some limitations because it needs to be installed and adjusted for height level. Computer vision is one potential approach for addressing these problems.

Recently, computer vision algorithms have been increasingly developed for rehabilitation, by applying image sensors such as Kinect and camera. However, the shoulder angle measurement data by Kinect or camera are reliable and valid when the sensor can clearly detect the position of the shoulder joint (Huber, Leeser, Sternad & Seitz, 2015; Huber, Seitz, Leeser, & Sternad, 2014). Therefore, image processing was used for the optimization of motion detection using a camera. Nonetheless, the quality of motion detection was better when using markers on the body part of interest of the human subject. Hence, this technique requires a specialist to place the markers. Consequently, the development of computer vision to detect images accurately without relying on the markers is a challenge, and is a promising approach to solving the problem. The previous studies have attempted to solve this problem by detecting shoulder movements without markers, using a computer vision system. Although this approach can detect the shoulder movement, it cannot measure the shoulder angle. Thus, the proposed system was applied to measure shoulder angle movement using computer vision with a web camera. The web camera is a non-invasive and non-contact sensor which is normally embedded in a laptop. In addition, the patients can measure their shoulder movement themselves anywhere and know the results instantly. Moreover, the data on the shoulder angle movement can be collected and analyzed for diagnosis, examination, and monitoring. Therefore, this method can measure the range of shoulder movements in a home-based rehabilitation program, and can provide expediency for patients who live far from their hospital or clinic.

## 2. Shoulder Angle Measurement System for Home-Based Rehabilitation

### 2.1 Shoulder Angle Measurement (SAM) system

The block diagram is shown in Figure 2 for the shoulder angle measurement in home-based rehabilitation. It consists of a clinician section and a patient section. The first

Figure 1. The usage of Thai Arthrometric Navigator Scale (TAN Scale): The top row is the shoulder flexion movement, and the bottom row is the shoulder abduction movement

section is for clinician, such as a doctor or a physical therapist. In this section, the clinician can set up a rehabilitation program for patients and interpret the range of shoulder angle movement data for follow-up and treatment plan. The configuration of the rehabilitation program is the action of movement, target and minimum angle, the number of times in 1 set, the number of sets in 1 day, and the number of days in 1 week. It will start when the patient signs in with HN number (Hospital number) and chooses an action of shoulder movement. After that, the camera starts capturing video frames for the shoulder angle measurement. These video frames are manipulated using computer vision techniques to segment an arm image. Then the arm image is analyzed for its orientation. Finally, the results on shoulder angle movement are saved and sent to the server.

### 2.2 Range of shoulder motion calculation

Range of shoulder motion calculation is in the patient section and involves the following steps. First, the configuration is set by a clinician. After that, the configuration is also displayed when patient signs in. Next, the shoulder angle measuring process is started. The angle measuring process is separated into 2 parts: the preparing part and the measuring part. In the preparing part, face image is detected by Viola-Jones technique. Rough shoulder position is determined from the face position and body segment length ratio (Azhar & Tjahjadi, 2014). For this experiment, the rough shoulder position is calculated for an individual participant. The details of calculation are described in section 3. The rough shoulder position is used to draw similar triangles for elbow flexion checking. The system collects the video frames to generate the initial background frame. During preparing time, the patient can take a rest and prepare to raise the arm. After the preparing time has ended, the measuring part starts. The moving object is detected by absolute differencing between the current frame and the background frame. Then the difference frame is compared with a threshold to segment the arm image. The segmented image is calculated using Equation (1). Next, the background frame is updated by

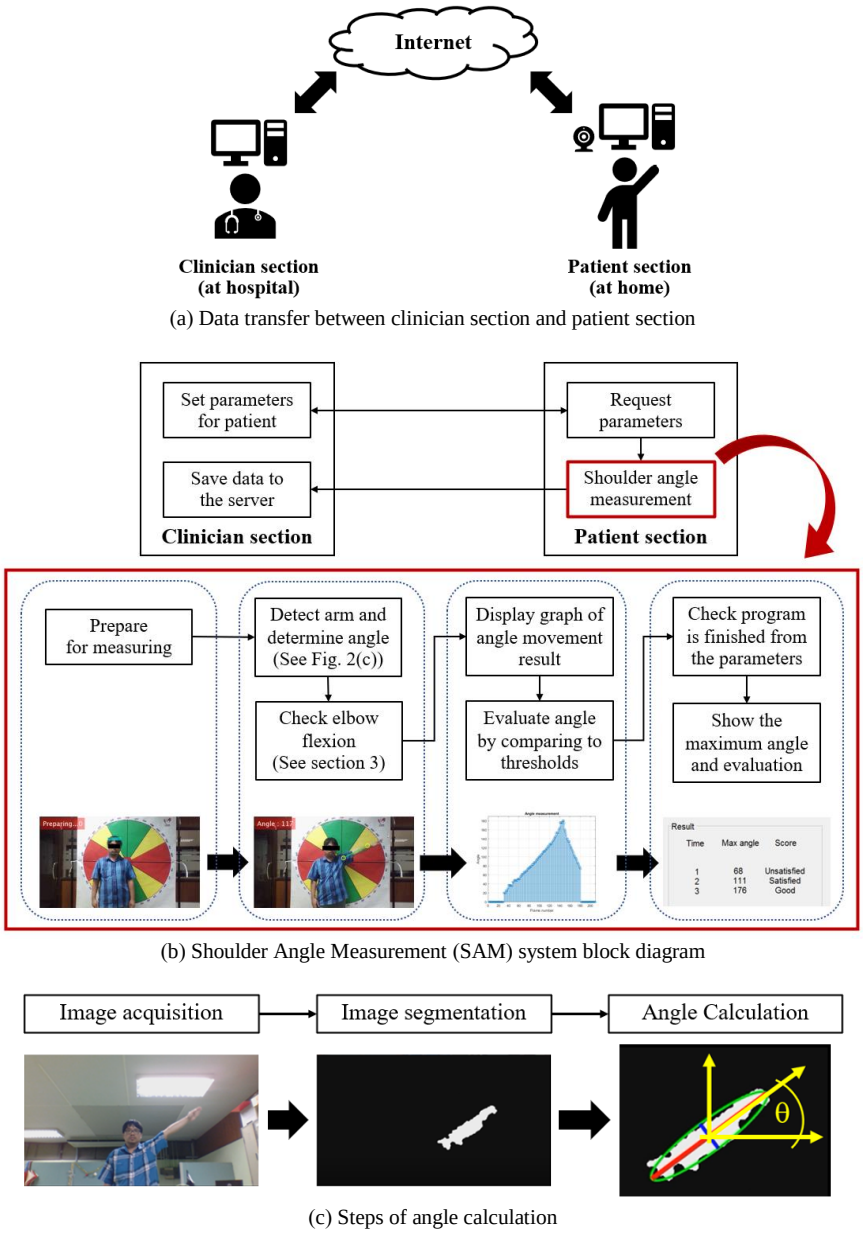


(a) Data transfer between clinician section and patient section

(b) Shoulder Angle Measurement (SAM) system block diagram

(c) Steps of angle calculation

Figure 2. Shoulder angle measurement system (SAM system)

learning rate (α) because the ambient background may be changing. An adaptive learning rate was applied to update the background frame, as in Equation (2) (Rungruangbaiyok, Duangsoithong, & Chetpattananondh, 2019).

$$D_t = \begin{cases} D_{x,y,t} = 1, if \ |F_{x,y,t} - B_{x,y,t}| \geq T_t \\ D_{x,y,t} = 0, Otherwise \end{cases} \quad (1)$$

where $F_{x,y,t}$ is the current frame, $B_{x,y,t}$ is the background frame, and $D_t$ is the segmented image frame. $D_{x,y,t} = 1$ means that the pixel $D_{x,y,t}$ is foreground, $D_{x,y,t} = 0$ means that the pixel $D_{x,y,t}$ is background, and $T_t$ is threshold that is determined by Gaussian Mixture Model.

$$B_{x,y,t} = \alpha F_{x,y,t-1} + (1 - \alpha) B_{x,y,t-1} \quad (2)$$

where $B_{x,y,t}$ is the background frame in the next frame, $B_{x,y,t-1}$ is the background frame in current frame, $F_{x,y,t-1}$ is the current frame, and α is the adaptive learning rate.

The segmented image is enhanced by a morphology technique. Then the angle of the arm image can be determined using image moment (*Mij*) by Equation (3). The detected arm image is a binary image. Hence, the values in the image are 0 (Black color) and 1 (White color).

$$M_{ij} = \iint x^i y^j f(x,y) dx dy \quad (3)$$

The zero-order moment ($M_{00}$) provides an area of the object image. The first-order moments ($M_{10}$ and $M_{01}$) normalized with $M_{00}$ provide the components of the centroids ($x_c$ and $y_c$). The second-order moments ($M_{20}$, $M_{11}$, and $M_{02}$) can form a covariance matrix of the arm image ($cov(I(x, y))$) as in Equation (4), and each element of the covariance matrix can be calculated from Equation (5) to Equation (7).

$$cov\big(I(x,y)\big) = \begin{bmatrix} \mu'_{20} & \mu'_{11} \\ \mu'_{11} & \mu'_{02} \end{bmatrix} \tag{4}$$

$$\mu'_{20} = \frac{M_{20}}{M_{00}} - x_c^2 \tag{5}$$

$$\mu'_{11} = \frac{M_{11}}{M_{00}} - x_c y_c \tag{6}$$

$$\mu'_{02} = \frac{M_{02}}{M_{00}} - y_c^2 \tag{7}$$

The eigenvectors of the covariance matrix correspond to the major and minor axes of the object image. Lengths of the major axis ($a$) and minor axis ($b$) can be calculated from from Equations (8) and (9).

$$a = 2 \times \sqrt{\frac{1}{2} \times \left(\mu'_{20} + \mu'_{02}\right) + \sqrt{4{\mu'_{11}}^2 + \left(\mu'_{20} - \mu'_{02}\right)^2}} \tag{8}$$

$$b = 2 \times \sqrt{\frac{1}{2} \times \left(\mu'_{20} + \mu'_{02}\right) - \sqrt{4{\mu'_{11}}^2 + \left(\mu'_{20} - \mu'_{02}\right)^2}} \tag{9}$$

The orientation ($\theta$) between the major axis of the arm image and X-axis is calculated in Equation (10). Hence, the image orientation can be determined, and the result is the angle of shoulder moment.

$$\theta = \frac{1}{2}\tan^{-1}\left(\frac{2\mu'_{11}}{\mu'_{20} - \mu'_{02}}\right) \tag{10}$$

According to the arm image orientation ($\theta'$), the result is compensated to evaluate shoulder range of motion for clinical evaluation in Equation (11).

$$\theta' = \begin{cases} 90 + \theta, & if\ x_h > x_s \\ 90 - \theta, & if\ x_h < x_s \\ 180, & if\ (x_h = x_s)\&(y_h > y_s) \\ 0, & Otherwise \end{cases} \tag{11}$$

where $x_h$ and $y_h$ are coordinates of the approximate hand position, and $x_s$ and $y_s$ are coordinates of the approximate shoulder position.

After compensation, the number of the measuring frames is checked. If the number of the measuring frames is less than the number of setting frames, the process will be done again until the number equals that of the setting frames. After that, the collected compensated result is displayed in a graph image. Next, the number of times in set is checked. If it is less than the number of setting times in one set, the process will be done again until the end of the number of times in one set. Then the maximum value of the shoulder angle movement result is selected to compare with degree of the minimum angle and target angle by Equation (12). Finally, the evaluated result is sent to a data server for evaluation and follow-up.

$$E = \begin{cases} Good, & if\ \theta' \geq \theta_{target} \\ Satisfied, & if\ \theta_{target} > \theta' \geq \theta_{min} \\ Unsatisfied, & \theta' < \theta_{min} \end{cases} \tag{12}$$

where $E$ is evaluated result, $\theta'$ is image orientation, $\theta_{target}$ and $\theta_{min}$ are target angle and minimum angle, respectively.

## 3. Elbow Flexion Checking

When the patient is raising hand for measuring, the movement may be a wrong type of motion, for example elbow flexion. Therefore, this section proposes a method to solve the problem. Normally, the displacement between shoulder point and fingertip is longer than the length of Bideltoid (Shoulder) breadth as shown in Figure 3(a). Consequently, there can be wrong motion checking when the patient is moving an arm. Nevertheless, the distance should be tuned for better checking, as displayed in Figure 3(b). In addition, pseudo code of the elbow flexion checking is sketched in Algorithm 1.

Algorithm 1. Elbow flexion checking

$D_F$ ← Distance between shoulder point and fingertip point (The fingertip point is assumed to be at the farthest pixel from shoulder point.)
$D_C$ ← Distance between chest point and shoulder point
$L$ ← Length of Shoulder breadth (It was approximate to 2 times of $D_C$)
$k$ ← Coefficient of $D_F$ (Tuning for optimized length)
if $L < kD_F$
    This movement cannot be an elbow flexion.
else
    This movement can be an elbow flexion.
end

The reference shoulder position is indexed by clinician at the first time to calculate chest ratio ($R_C$) and shoulder ratio ($R_S$). Then the ratios will be applied for the next time. The wrong motion that is elbow flexion can be checked by these following steps. First, the shoulder position is assigned by clinician (The position at the point S in Figure 3(c)). The second step is that the middle point of the detected face image is determined. After that, the similar triangles (ΔFCS and ΔFXY) are generated as shown in Figure 3(c). Corresponding angles of similar triangles (ΔFCS and ΔFXY) are equal while the line XY moves parallel to the line CS. Therefore, size of detected face image box does not affect the ratios. The line XY is at bottom edge of detected face image box, and point F is the middle point of detected face image. Point S is an assigned shoulder point. Point C is assumed to be a chest point. It is an intersection point between vertical line passing through point F and horizontal line passing through

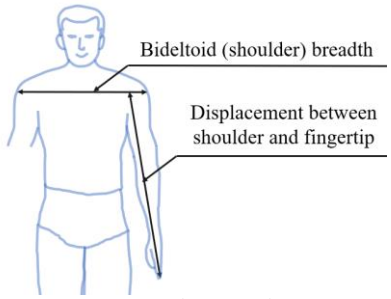


(a) Body section length for elbow flexion checking

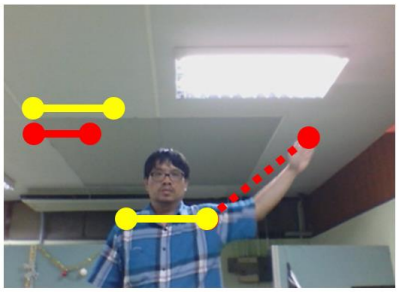

)b( Distance comparison: the red dashed line is distance between shoulder point and fingertip, the red solid line is downsized distance of the red dashed line, and the yellow solid line is shoulder breadth length.

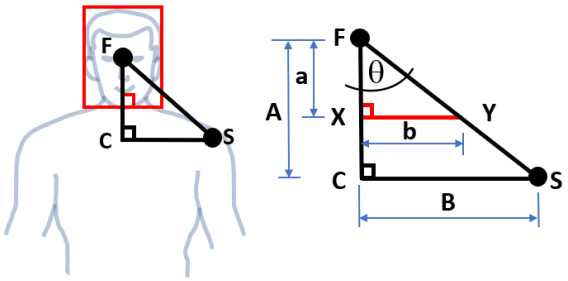


(c) Similar triangles for chest ratio and shoulder ratio calculation

Figure 3. Elbow flexion checking

point S. Additionally, angles in ΔFCS are constant while scale of the triangle is varied. Hence, this feature can determine a rough shoulder position. Similarly, the shoulder ratio ($R_S$) is a tangent value at point F by Equation (13). Chest ratio ($R_C$) is obtained from Equation (14) that is transformed by Equation (14). When measuring, the ratios will determine the shoulder position by the following steps. First, distance a is obtained by calculation from face image box. After that, distance $A$ is calculated by Equation (15). Next, distance $B$ is determined by Equation (16). Finally, the shoulder position ($S(x,y)$) is gotten from Equation (17). Nonetheless, the assigned position should be close to the real position.

$$R_S = \frac{B}{A} = \frac{b}{a} \tag{13}$$

$$R_C = \frac{a}{A} = \frac{b}{B} \tag{14}$$

$$A = \frac{a}{R_C} \tag{15}$$

$$B = A \times R_S \tag{16}$$

$$S(x,y) = S(F_x + B, F_y + A) \tag{17}$$

where $a$, $b$, $A$, and $B$ are lengths of corresponding sides of similar triangles. $F(x,y)$ is the coordinates of the middle point of face box.

## 4. Experimental Result

### 4.1 Experimental Setup

The experiment was set in an indoor room, and the illumination was not changed suddenly. The illumination was 400 lux from 6 sets of surface louver luminaire with 2x36 Watt fluorescents in the room that has dimensions of 7 x 8 x 2.7 $m^3$. Ten healthy participants (Height = 172.5 ± 7.4 cm., chest width = 46.3 ± 5.7 cm., distance between shoulder and finger = 67.8 ± 1.33 cm.) participated in the measurements of a preliminary study. Each participant stood in front of a laptop camera. Distance between participant and camera was 3.5 m in order to record the upper body of the participant. Additionally, guiding area can be set for ensuring position in a suitable range, as illustrated in Figure 4(a). The participants measured angles for four movements without elbow flexion: Left shoulder abduction (LSA), Right shoulder abduction (RSA), Left shoulder flexion (LSF), and right shoulder flexion (RSF). The positions at 10 and 20 degrees were not tested because these positions were close to the body. Therefore, they may be occluded, and might not match the adapted TAN Scale (ATAN Scale). The original TAN Scale was expanded to a range from 0 to 180 degrees. The rest of the angles, every 10 degrees from 30 to 180-degree, were recorded in 50 samples per each movement.

The relation among the two compared methods is shown in boxplot because this graph type can show statistical results, such as mean and standard deviation. The correlation study between the SAM system and the two other devices: ATAN Scale, and goniometer, used Pearson correlations and linear regression. Performance of the SAM system was determined by full-scale error (*%FS*), and 95% confidence interval (95% CI). The full-scale error was determined using Equation (19).

$$\%FS = \frac{|\theta_{Actual} - \theta_{Ideal}|}{180} \times 100 \tag{19}$$

where $\%FS$ is the full-scale error, $\theta_{Actual}$ is the actual measured angle, and $\theta_{Ideal}$ is the ideal measured angle.

Before measuring, parameters of configuration were set. Then participant filled up HN number, action movement to sign in. After that, the graphical user interface (GUI) gave information, such as degree of minimum angle and target angle. Finally, measuring shoulder angle movements was started. An example of the GUI is shown in Figure 4(b).

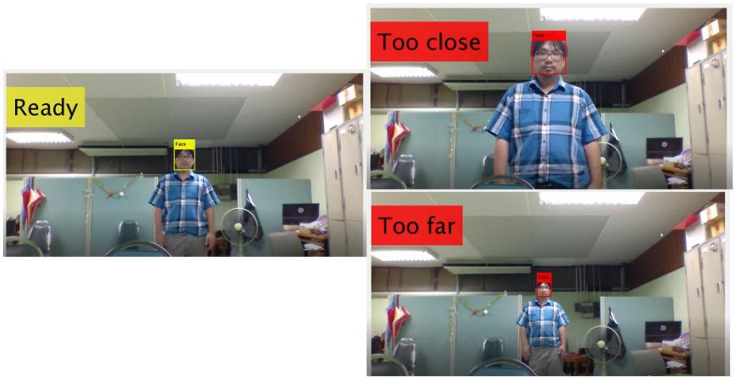


(a) Guiding area for measurement

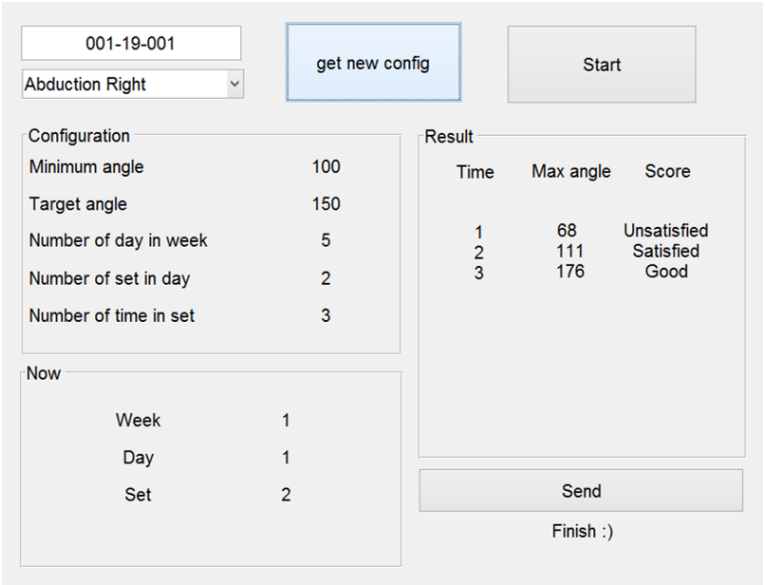


(b) Graphical user interface

Figure 4. The proposed system in patient section

## 4.2 Results

The face image was detected, and the rough shoulder position was determined. Then the angle of shoulder movement was calculated during the measuring time section. After that, graph of the result was displayed as in Figure 5. Furthermore, the maximum angle results were sent to the server. Clinicians can evaluate and monitor the results at hospital, while the patient performed the movements at home, as shown in Figure 6. The maximum angle results with the minimum threshold (the red line) and target threshold (the green line) are displayed in Figure 6(a). The collected data are illustrated in Figure 6(b). Hence, clinicians can follow-up by evaluation of results and by design of a treatment plan.

The ATAN Scale and the proposed system had an approximate relationship. Pearson correlations between measured angles using the SAM system and the ATAN Scale of LSA, RSA, LSF, and RSF were 0.9977, 0.9978, 0.9975, and 0.9986, respectively. Boxplots in Figure 7(a) - 7(d) show the statistical results of the SAM system, which was compared to the ATAN Scale. The measuring results between 1$^{st}$ quartile and 3$^{rd}$ quartile covered the target angle. The linear regression results are shown in Figures 7(e) - 7(h). When the linear regression was applied to all results, the coefficients of determination $r^2$ of LSA, RSA, LSF, and RSF were 0.9954, 0.9956, 0.9951, and 0.9972, respectively. The slopes of the linear regression line were 0.973, 0.977,0.963, and 0.976, respectively. Table 1 summarizes the results from comparing the proposed system with the ATAN Scale. The maximum full-scale error was 5.03 at the 180-degree position. However, the maximum error in the range between 30 and 170 degree positions was less than 3. Most of the target degrees were in the middle of the upper and lower 95% confidence interval bounds.

In another comparison, Pearson correlations between the measured angles using the SAM system and a goniometer of LSA, RSA, LSF, and RSF were 0.9972, 0.9975, 0.9966, and 0.9974, respectively. Boxplots in Figure 8(a) – 8(d) show the statistical results of the SAM system when compared to the goniometer. The target angles were intervals between 1$^{st}$ quartile and 3$^{rd}$ quartile of the measuring results. The linear regression results are illustrated in Figures 8(e) –

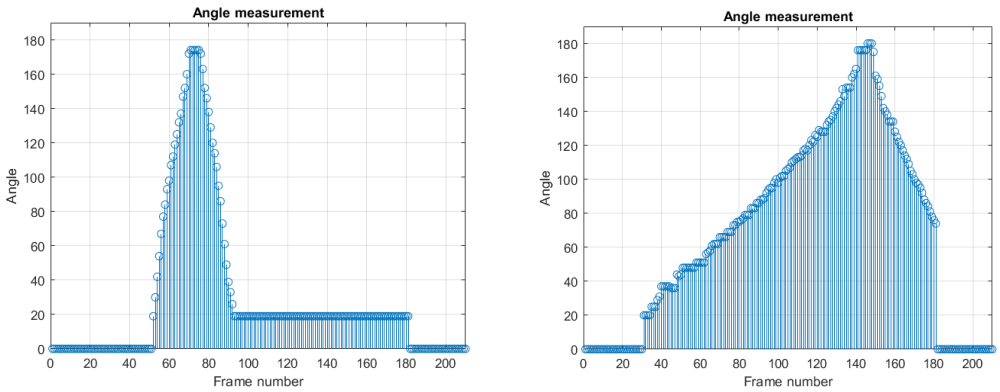


(a) Fast moving (b) Slow moving

Figure 5. Angle measurement results and comparison of fast and slow movements

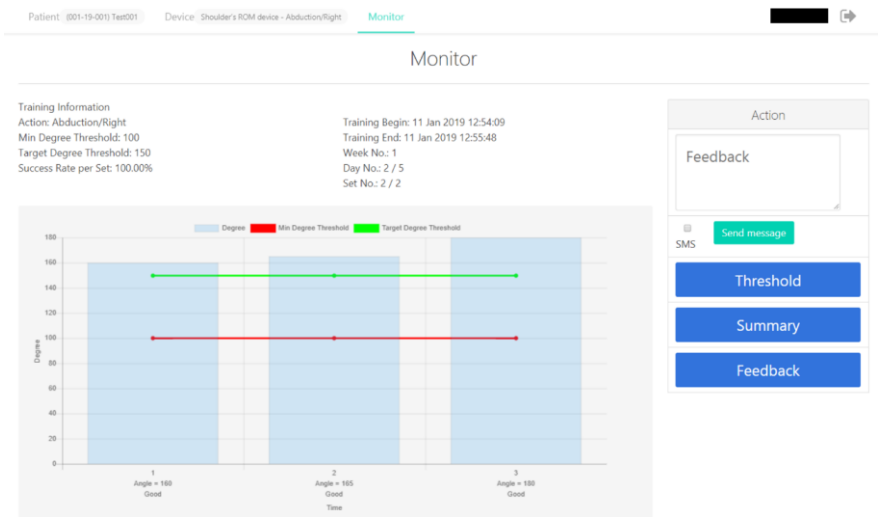


(a) Evaluation

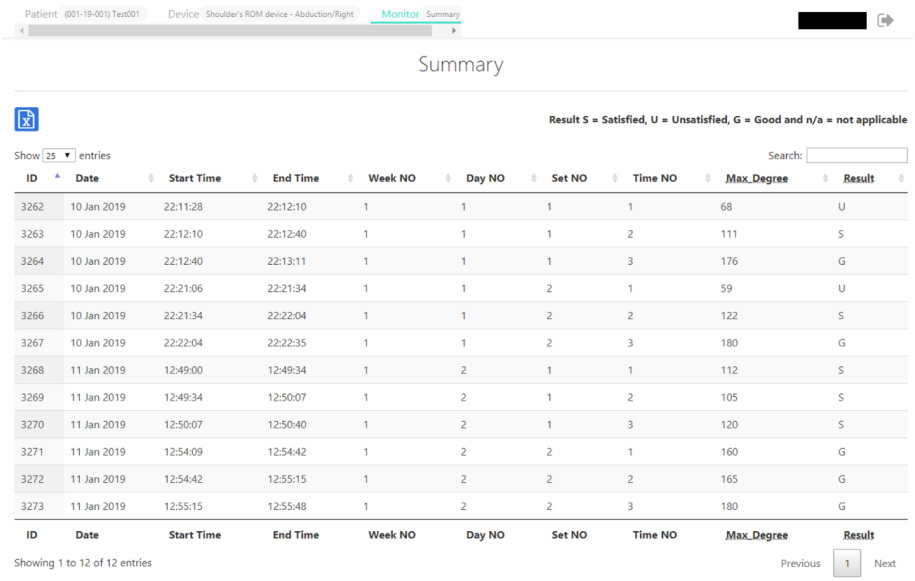


| ID | Date | Start Time | End Time | Week NO | Day NO | Set NO | Time NO | Max_Degree | Result |
|---|---|---|---|---|---|---|---|---|---|
| 3262 | 10 Jan 2019 | 22:11:28 | 22:12:10 | 1 | 1 | 1 | 1 | 68 | U |
| 3263 | 10 Jan 2019 | 22:12:10 | 22:12:40 | 1 | 1 | 1 | 2 | 111 | S |
| 3264 | 10 Jan 2019 | 22:12:40 | 22:13:11 | 1 | 1 | 1 | 3 | 176 | G |
| 3265 | 10 Jan 2019 | 22:21:06 | 22:21:34 | 1 | 1 | 2 | 1 | 59 | U |
| 3266 | 10 Jan 2019 | 22:21:34 | 22:22:04 | 1 | 1 | 2 | 2 | 122 | S |
| 3267 | 10 Jan 2019 | 22:22:04 | 22:22:35 | 1 | 1 | 2 | 3 | 180 | G |
| 3268 | 11 Jan 2019 | 12:49:00 | 12:49:34 | 1 | 2 | 1 | 1 | 112 | S |
| 3269 | 11 Jan 2019 | 12:49:34 | 12:50:07 | 1 | 2 | 1 | 2 | 105 | S |
| 3270 | 11 Jan 2019 | 12:50:07 | 12:50:40 | 1 | 2 | 1 | 3 | 120 | S |
| 3271 | 11 Jan 2019 | 12:54:09 | 12:54:42 | 1 | 2 | 2 | 1 | 160 | G |
| 3272 | 11 Jan 2019 | 12:54:42 | 12:55:15 | 1 | 2 | 2 | 2 | 165 | G |
| 3273 | 11 Jan 2019 | 12:55:15 | 12:55:48 | 1 | 2 | 2 | 3 | 180 | G |



(b) Monitoring

Figure 6. The graphical user interface for evaluation and monitoring

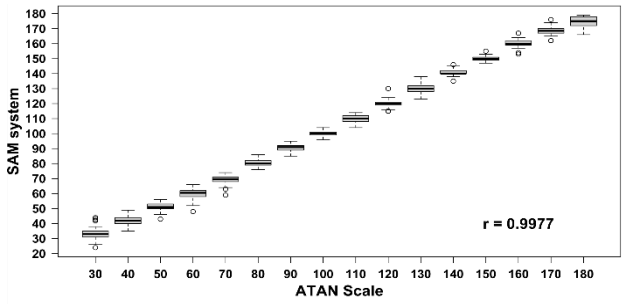


(a) Left shoulder abduction

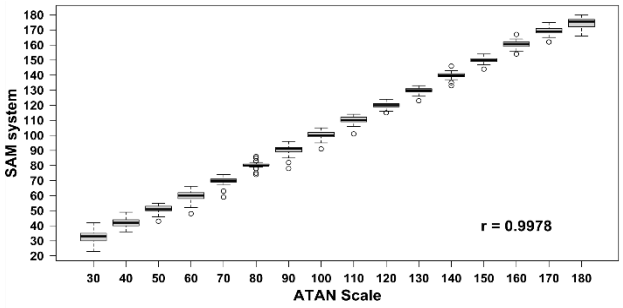


(b) Right shoulder abduction

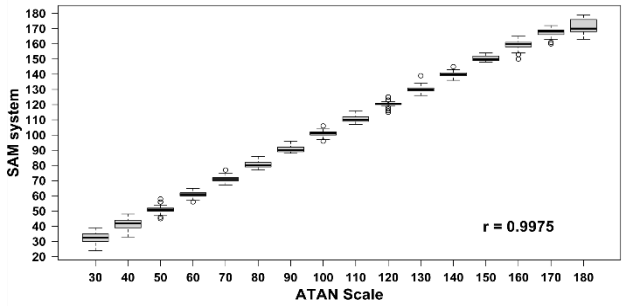


(c) Left shoulder flexion

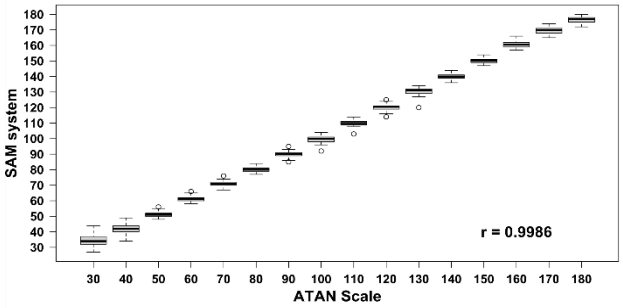


(d) Right shoulder flexion

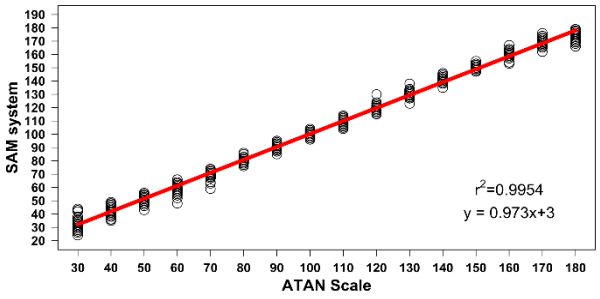


(e) Left shoulder abduction

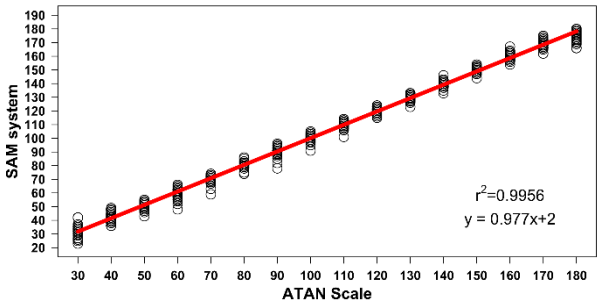


(f) Right shoulder abduction

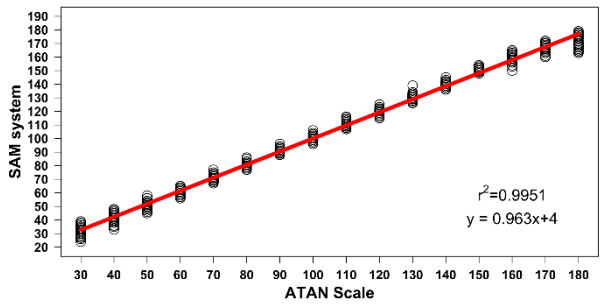


(g) Left shoulder flexion

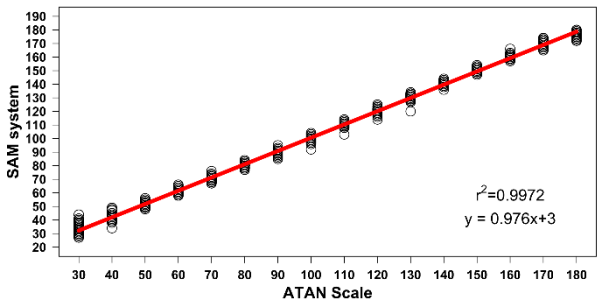


(h) Right shoulder flexion

Figure 7. Linear regression and boxplots of the SAM system versus ATAN Scale

8(h). When linear regression was applied to all results, it showed that $r^2$ of LSA, RSA, LSF, and RSF were 0.9943, 0.9950, 0.9931, and 0.9948, respectively. The slopes of the linear regression line were 0.974, 0.981, 0.983, and 0.985, respectively. Table 2 summarizes comparison of the proposed system with the goniometer. The maximum full-scale error was 3.69 at the 180 degrees position. Nevertheless, the maximum error in the range between the 30 to 170-degree position was less than 3. Most of the target degrees were also in the middle of the upper and lower of 95% confidence interval bounds.

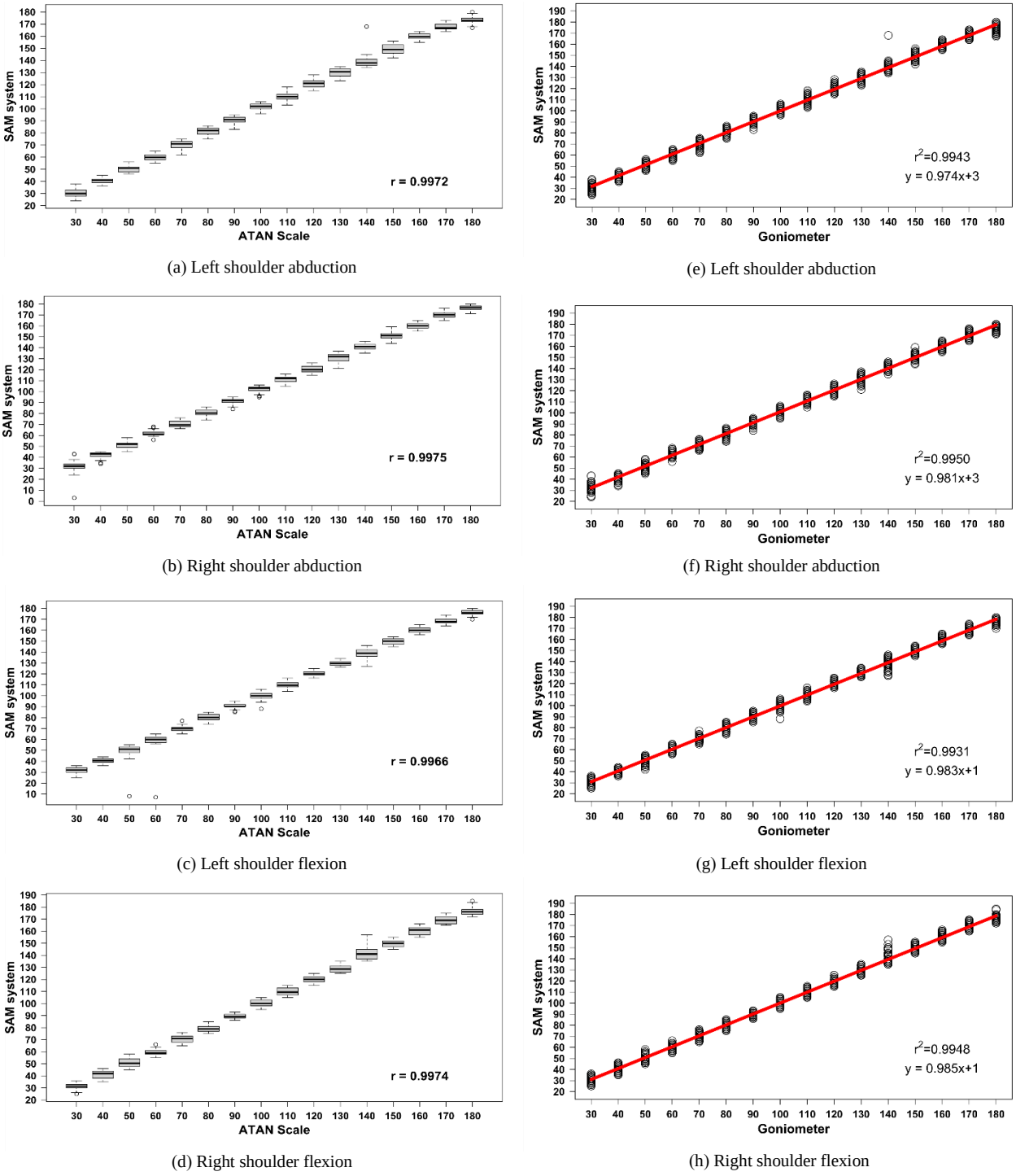


(a) Left shoulder abduction

(e) Left shoulder abduction

(b) Right shoulder abduction

(f) Right shoulder abduction

(c) Left shoulder flexion

(g) Left shoulder flexion

(d) Right shoulder flexion

(h) Right shoulder flexion

Figure 8. Linear regression and boxplots of the SAM system versus goniometer

## 5. Discussion

Pearson correlations of the SAM system with the two reference devices (ATAN Scale and goniometer) were close to one. In addition, linear regression slopes were also close to one. This indicates that the proposed measurement system and the two reference devices were well correlated. Besides, elbow flexion during measuring can be detected. Accordingly, the proposed system can be used instead of the TAN Scale or the goniometer. Moreover, the SAM system may be applied with many diseases or sport injuries that might cause shoulder impairments. Nonetheless, the results may be inaccurate because of arm images that are not detected perfectly. One of the factors that can impact arm image

Table 1. The angle measurement result when comparing to ATAN Scale

| | degree | 30 | 40 | 50 | 60 | 70 | 80 | 90 | 100 | 110 | 120 | 130 | 140 | 150 | 160 | 170 | 180 |
|---|---|---|---|---|---|---|---|---|---|---|---|---|---|---|---|---|---|
| Left abduction | Mean | 33.40 | 42.16 | 51.46 | 60.08 | 69.36 | 80.40 | 90.50 | 100.12 | 109.78 | 119.94 | 130.22 | 140.68 | 150.22 | 160.32 | 168.64 | 174.42 |
| | Sd | 4.38 | 3.59 | 2.50 | 3.37 | 2.68 | 2.040 | 2.18 | 1.96 | 2.47 | 2.52 | 2.63 | 1.85 | 1.68 | 2.61 | 2.61 | 3.89 |
| | *% FS* | 2.36 | 1.89 | 1.23 | 1.40 | 1.04 | 0.87 | 0.99 | 0.87 | 1.06 | 0.94 | 1.14 | 0.73 | 0.68 | 1.04 | 1.27 | 3.10 |
| | %$CI_{up}$ | 32.15 | 41.14 | 50.75 | 59.12 | 68.6 | 79.82 | 89.88 | 99.56 | 109.08 | 119.22 | 129.47 | 140.16 | 149.74 | 159.58 | 167.90 | 173.31 |
| | %$CI_{low}$ | 34.65 | 43.18 | 52.17 | 61.04 | 70.12 | 80.98 | 91.12 | 100.68 | 110.48 | 120.66 | 130.97 | 141.20 | 150.70 | 161.06 | 169.38 | 175.53 |
| Right abduction | Mean | 32.36 | 42.12 | 50.82 | 59.62 | 69.64 | 80.42 | 90.54 | 100.18 | 110.14 | 120.06 | 129.88 | 139.92 | 150.18 | 160.34 | 169.00 | 174.60 |
| | Sd | 4.45 | 3.48 | 2.32 | 3.43 | 2.51 | 2.03 | 3.18 | 2.37 | 2.36 | 1.78 | 2.01 | 2.22 | 1.80 | 2.29 | 2.60 | 3.88 |
| | *% FS* | 2.29 | 1.73 | 1.03 | 1.48 | 0.91 | 0.79 | 1.28 | 0.94 | 0.97 | 0.72 | 0.82 | 0.89 | 0.72 | 0.97 | 1.16 | 3.00 |
| | %$CI_{up}$ | 31.09 | 41.13 | 50.16 | 58.64 | 68.93 | 79.84 | 89.64 | 99.51 | 109.47 | 119.55 | 129.31 | 139.29 | 149.67 | 159.69 | 168.26 | 173.50 |
| | %$CI_{low}$ | 33.63 | 43.11 | 51.48 | 60.60 | 70.35 | 81.00 | 91.44 | 100.85 | 110.81 | 120.57 | 130.45 | 140.55 | 150.69 | 160.99 | 169.74 | 175.70 |
| Left flexion | Mean | 32.04 | 41.54 | 51.08 | 60.92 | 71.08 | 80.48 | 90.70 | 100.64 | 110.56 | 120.42 | 130.22 | 139.98 | 150.32 | 159.44 | 167.36 | 170.94 |
| | Sd | 3.57 | 3.25 | 2.51 | 2.15 | 1.96 | 1.95 | 1.93 | 1.79 | 2.22 | 1.90 | 2.07 | 1.65 | 1.68 | 2.74 | 2.75 | 4.73 |
| | *% FS* | 1.93 | 1.59 | 1.09 | 1.00 | 0.93 | 0.82 | 0.86 | 0.76 | 0.93 | 0.77 | 0.74 | 0.68 | 0.76 | 1.07 | 1.56 | 5.03 |
| | %$CI_{up}$ | 31.02 | 40.62 | 50.37 | 60.31 | 70.52 | 79.93 | 90.15 | 100.13 | 109.93 | 119.88 | 129.63 | 139.51 | 149.84 | 158.66 | 166.58 | 169.6 |
| | %$CI_{low}$ | 33.06 | 42.46 | 51.79 | 61.53 | 71.64 | 81.03 | 91.25 | 101.15 | 111.19 | 120.96 | 130.81 | 140.45 | 150.80 | 160.22 | 168.14 | 172.28 |
| Right flexion | Mean | 34.36 | 42.14 | 51.08 | 60.86 | 71.00 | 80.18 | 89.96 | 99.64 | 110.18 | 120.22 | 130.36 | 140.2 | 150.36 | 160.58 | 169.84 | 176.54 |
| | Sd | 3.92 | 3.00 | 1.87 | 1.77 | 1.86 | 1.71 | 1.84 | 2.07 | 1.77 | 2.06 | 2.30 | 1.63 | 1.56 | 1.72 | 2.32 | 2.19 |
| | *% FS* | 2.60 | 1.54 | 0.91 | 0.83 | 0.93 | 0.72 | 0.76 | 0.82 | 0.70 | 0.90 | 0.96 | 0.67 | 0.71 | 0.77 | 1.07 | 1.92 |
| | %$CI_{up}$ | 33.25 | 41.20 | 50.55 | 60.36 | 70.47 | 79.69 | 89.44 | 99.05 | 109.68 | 119.63 | 129.71 | 139.74 | 149.92 | 160.09 | 169.18 | 175.92 |
| | %$CI_{low}$ | 35.47 | 42.99 | 51.61 | 61.36 | 71.53 | 80.67 | 90.48 | 100.23 | 110.68 | 120.81 | 131.01 | 140.66 | 150.80 | 161.07 | 170.50 | 177.16 |

Table 2. The angle measurement result when comparing to goniometer

| | degree | 30 | 40 | 50 | 60 | 70 | 80 | 90 | 100 | 110 | 120 | 130 | 140 | 150 | 160 | 170 | 180 |
|---|---|---|---|---|---|---|---|---|---|---|---|---|---|---|---|---|---|
| Left abduction | Mean | 30.66 | 40.40 | 50.60 | 60.02 | 70.44 | 81.34 | 90.90 | 101.94 | 109.90 | 120.76 | 130.12 | 139.16 | 149.16 | 159.56 | 167.80 | 173.36 |
| | Sd | 3.28 | 2.36 | 2.60 | 2.49 | 3.61 | 2.85 | 2.60 | 2.73 | 3.38 | 2.90 | 3.05 | 5.00 | 3.57 | 2.64 | 2.70 | 2.75 |
| | *% FS* | 1.46 | 1.11 | 1.27 | 1.08 | 1.71 | 1.50 | 1.21 | 1.59 | 1.50 | 1.36 | 1.44 | 1.76 | 1.78 | 1.22 | 1.64 | 3.69 |
| | %$CI_{up}$ | 29.73 | 39.73 | 49.86 | 59.31 | 69.41 | 80.53 | 90.16 | 101.16 | 108.94 | 119.93 | 129.25 | 137.74 | 148.15 | 158.81 | 167.03 | 172.58 |
| | %$CI_{low}$ | 31.59 | 41.07 | 51.34 | 60.73 | 71.47 | 82.15 | 91.64 | 102.72 | 110.86 | 121.59 | 130.99 | 140.58 | 150.17 | 160.31 | 168.57 | 174.14 |
| Right abduction | Mean | 31.70 | 41.86 | 51.42 | 61.76 | 70.22 | 80.82 | 91.10 | 101.98 | 111.52 | 120.50 | 130.88 | 140.86 | 150.92 | 159.84 | 169.92 | 176.18 |
| | Sd | 5.74 | 2.85 | 2.96 | 2.22 | 2.95 | 2.90 | 2.36 | 2.71 | 2.64 | 3.21 | 3.45 | 2.48 | 2.83 | 2.63 | 3.04 | 2.46 |
| | *% FS* | 2.26 | 1.70 | 1.61 | 1.18 | 1.39 | 1.34 | 1.17 | 1.63 | 1.44 | 1.57 | 1.69 | 1.17 | 1.33 | 1.20 | 1.38 | 2.12 |
| | %$CI_{up}$ | 30.07 | 41.05 | 50.58 | 61.13 | 69.38 | 79.99 | 90.43 | 101.21 | 110.77 | 119.59 | 129.90 | 140.15 | 150.11 | 159.09 | 169.06 | 175.48 |
| | %$CI_{low}$ | 33.33 | 42.67 | 52.26 | 62.39 | 71.06 | 81.65 | 91.77 | 102.75 | 112.27 | 121.41 | 131.86 | 141.57 | 151.73 | 160.59 | 170.78 | 176.88 |
| Left flexion | Mean | 31.46 | 40.52 | 49.70 | 59.06 | 69.64 | 80.16 | 90.72 | 100.08 | 109.72 | 120.42 | 129.66 | 138.32 | 149.58 | 159.96 | 168.26 | 175.94 |
| | Sd | 2.83 | 2.14 | 6.73 | 7.96 | 2.25 | 2.99 | 2.15 | 3.30 | 2.70 | 2.33 | 2.34 | 4.99 | 2.56 | 2.66 | 2.35 | 2.11 |
| | *% FS* | 1.54 | 1.02 | 1.90 | 1.79 | 0.96 | 1.40 | 0.93 | 1.38 | 1.24 | 1.08 | 1.06 | 2.22 | 1.19 | 1.24 | 1.32 | 2.26 |
| | %$CI_{up}$ | 30.66 | 39.61 | 47.79 | 56.80 | 69.00 | 79.31 | 90.11 | 99.14 | 108.95 | 119.76 | 129.00 | 136.90 | 148.85 | 159.20 | 167.59 | 175.34 |
| | %$CI_{low}$ | 32.26 | 41.13 | 51.61 | 61.32 | 70.28 | 81.01 | 91.33 | 101.02 | 110.49 | 121.08 | 130.32 | 139.74 | 150.31 | 160.72 | 168.93 | 176.54 |
| Right flexion | Mean | 31.32 | 41.20 | 50.96 | 59.44 | 70.56 | 79.16 | 89.46 | 99.88 | 109.92 | 120.14 | 128.72 | 141.64 | 149.50 | 160.12 | 169.44 | 176.22 |
| | Sd | 2.58 | 3.19 | 3.45 | 2.54 | 3.02 | 2.79 | 1.80 | 3.06 | 3.16 | 3.04 | 3.08 | 5.01 | 2.88 | 3.38 | 3.51 | 2.64 |
| | *% FS* | 1.31 | 1.64 | 1.64 | 1.13 | 1.40 | 1.33 | 0.86 | 1.47 | 1.56 | 1.39 | 1.56 | 2.29 | 1.32 | 1.67 | 1.71 | 2.30 |
| | %$CI_{up}$ | 30.59 | 40.29 | 49.98 | 58.72 | 69.70 | 78.37 | 88.95 | 99.01 | 109.02 | 119.28 | 127.85 | 140.22 | 148.68 | 159.16 | 168.44 | 175.47 |
| | %$CI_{low}$ | 32.05 | 42.11 | 51.94 | 60.16 | 71.42 | 79.95 | 89.97 | 100.75 | 110.82 | 121.00 | 129.59 | 143.06 | 150.32 | 161.08 | 170.44 | 176.97 |

detection is illumination. Although this experiment was set in a room in which the illumination did not change quickly, the background might have some effects, due to its shadows and reflections.

Graphing the results displayed the shoulder angle movement in sequence over every frame. The slope of timeprofile of the angle shows speed of the movement when a participant raised the arm, as seen in Figure 5. For instance, the slope of the result in Figure 5(a) was greater than in Figure 5(b). Hence, the movement in Figure 5(a) was faster than in Figure 5(b). Furthermore, the angle results in Figure 5(a) remained in 20 degree from the number of frames was 90 to 180 because the results shown are the last results if the participant does not move for a while. Consequently, this graph did not only show the shoulder angle movement, but it also illustrated the maximum angle that was calculated for evaluation, and how the subject moved, as regards the speed.

The first limitation of the proposed system is that only one person should be in front of the web camera, because the system does not recognize who is the intended subject. The second limitation is that the subject should stand up straight, without lateral bending while measuring, because the angle result could otherwise be wrong. These 2 limitations will be addressed in future work.

## 6. Conclusions

Impaired shoulder movement patients who live far from a hospital can have difficulties in getting follow-up care from a doctor. Therefore, this paper proposes a shoulder angle measurement (SAM) system for homebased rehabilitation, implemented by using a common web camera. The system can estimate the angle of shoulder movement and send the results to a clinician. The maximum full-scale error was 5.03, and 3.69 when comparing to the ATAN Scale, and to a goniometer, respectively. Furthermore, the two reference devices can be replaced with the SAM system because of highly correlated measurement results. However, the SAM system has some limitations that will be addressed in further work.

## Acknowledgements

This research was funded by the Broadcasting and Telecommunications Research and Development Fund for the Public Interest (BTFP), Office of The National Broadcasting and Telecommunications Commission (NBTC). The Department of Physical Therapy, Faculty of Medicine, Prince of Songkla University, the Department of Electrical Engineering, Faculty of Engineering, Prince of Songkla University, PSU-Ph.D. Scholarship, and Prince of Songkla University for Graduate School Dissertation Funding for Thesis are gratefully acknowledged for support. In addition, the authors would like to thank anonymous reviewers for their valuable comments.

## References

Azhar, F., & Tjahjadi, T. (2014). Significant body point labeling and tracking. *IEEE Transactions on Cybernetics*, *44*(9), 1673-1685. doi:10.1109/TCYB.2014.2303993

Box, R. C., Reul-Hirche, H. M., Bullock-Saxton, J. E., & Furnival, C. M. (2002). Shoulder movement after breast cancer surgery: Results of a randomised controlled study of postoperative physiotherapy. *Breast Cancer Research and Treatment*, *75*(1), 35-50. doi:10.1023/a:1016571204924

Cao, Z., Simon, T., Wei, S. E., & Sheikh, Y. (2017). Realtime multi-person 2d pose estimation using part affinity fields. *Proceedings of the IEEE Conference on Computer Vision and Pattern Recognition* (pp. 7291-7299). doi:10.1109/CVPR.2017.143

Chiensriwimol, N., Chan, J. H., Mongkolnam, P., & Mekhora, K. (2017). Monitoring frozen shoulder exercises to support clinical decision on treatment process using smartphone. *Procedia Computer Science*, *111*, 129-136. doi:10.1016/j.procs.2017.06.019

de Carlos-Iriarte, E., Mosquera-González, M., Alonso-García, M., Andrés-Prado, M., Machota-Blas, E., Hernández-García, J., & Rodríguez-Caravaca, G. (2019). Upper-limb morbidity in patients undergoing a rehabilitation program after breast cancer surgery: A 10-year follow-up study. *Rehabilitation Oncology*, 37(2), 70-76. doi:10.1097/01.REO.0000000000000131

Dougherty, J., Walmsley, S., & Osmotherly, P. G. (2015). Passive range of movement of the shoulder: a standardized method for measurement and assessment of intrarater reliability. *Journal of Manipulative and Physiological Therapeutics*, *38*(3), 218-224. doi:10.1016/j.jmpt.2014.11.006

Flores, A. M., & Dwyer, K. (2014). Shoulder impairment before breast cancer surgery. *Journal of Women's Health Physical Therapy*, *38*(3), 118. doi:10.1097/JWH.0000000000000020

Ghazal, S., & Khan, U. S. (2018, March). Human posture classification using skeleton information. *2018 IEEE International Conference on Computing, Mathematics and Engineering Technologies (iCoMET)* (pp. 1-4). doi:10.1109/ICOMET.2018.8346407

Hidding, J. T., Beurskens, C. H., van der Wees, P. J., van Laarhoven, H. W., & Nijhuis van der Sanden, M. W. (2014). Treatment related impairments in arm and shoulder in patients with breast cancer: A systematic review. *PloS one*, *9*(5). doi:10.1371/journal.pone.0096748

Huang, M. C., Lee, S. H., Yeh, S. C., Chan, R. C., Rizzo, A., Xu, W., . . . Shan-Hui, L. (2014). Intelligent frozen shoulder rehabilitation. *IEEE Intelligent Systems*, *29*(3), 22-28. doi:10.1109/MIS.2014.35

Huber, M. E., Seitz, A. L., Leeser, M., & Sternad, D. (2014, April). Validity and reliability of Kinect for measuring shoulder joint angles. *2014 IEEE 40th Annual Northeast Bioengineering Conference (NEBEC)* (pp. 1-2). doi:10.1109/NEBEC.2014.6972818

Huber, M., Leeser, M., Sternad, D., & Seitz, A. L. (2015). Accuracy of Kinect for measuring shoulder joint angles in multiple planes of motion. *2015 IEEE International Conference on Virtual Rehabilitation (ICVR)* (pp. 170-171). doi:10.1109/ICVR.2015.7358612

Kootstra, J. J., Dijkstra, P. U., Rietman, H., de Vries, J., Baas, P., Geertzen, J. H., . . . Hoekstra-Weebers, J. E. (2013). A longitudinal study of shoulder and arm morbidity in breast cancer survivors 7 years after sentinel lymph node biopsy or axillary lymph node dissection. *Breast Cancer Research and Treatment*, 139(1), 125-134. doi:10.1007/s10549-013-2509-y

Kumar, R. R. P., Muknahallipatna, S., McInroy, J., McKenna, M., & Franc, L. (2017). Real-time range of motion measurement of physical therapeutic exercises. *Journal of Computer and Communications*, *5*(9), 19-42. doi:10.4236/jcc.2017.59003

Mangal, N. K., Pal, S., & Khosla, A. (2017). Frozen shoulder rehabilitation using microsoft kinect. *2017 IEEE International Conference on Innovations in Green Energy and Healthcare Technologies (IGEHT)* (pp. 1-6). doi:10.1109/IGEHT.2017.8094043

Matsen III, F. A., Lauder, A., Rector, K., Keeling, P., & Cherones, A. L. (2016). Measurement of active shoulder motion using the Kinect, a commercially available infrared position detection system. *Journal of Shoulder and Elbow Surgery*, *25*(2), 216-223. doi:10.1016/j.jse.2015.07.011

National Cancer Institute, Department of Medical Services, Ministry of Public Health Thailand. *The Manual of Thai Arthrometric Navigator Scale (TAN Scale)*. Retrieved from http://www.nci.go.th/th/images/image_index/tanscale/ART%20ok.pdf

Ongvisatepaiboon, K., Chan, J. H., & Vanijja, V. (2015). Smartphone based tele-rehabilitation system for frozen shoulder using a machine learning approach. *2015 IEEE Symposium Series on Computational Intelligence* (pp. 811-815). doi:10.1109/SSCI.2015.120

Rungruangbaiyok, S., Duangsoithong, R., & Chetpattana nondh, K. (2019). Probabilistic static foreground elimination for background subtraction. *The Imaging Science Journal*, *67*(7), 385-395. doi:10.1080/13682199.2019.1672849

Yodpijit, N., Jongprasithporn, M., Saengmanee, S., Suriyapen, P., Imsamran, W., Chaiwerawattana, A., . . . Choosanit, P. (2018). The Thai Arthrometric Navigator (TAN) scale smartphone application for cancer patients. *2018 IEEE 4th International Conference on Control, Automation and Robotics (ICCAR)* (pp. 509-513). doi:10.1109/iccar.2018.8384729